Self-Aligned Tetrahedral Blade Architecture for Hybrid Lift–Drag VAWT

A Geometrically Self-Aligned Tetrahedral Blade Architecture for Hybrid Lift–Drag Vertical-Axis Wind Turbines

YoungJune Jeon GeoWind

Abstract

Background. Hybrid lift–drag vertical-axis wind turbines (VAWTs) bridge the operating envelopes of pure drag-type (Savonius) and pure lift-type (Darrieus) machines, but conventional implementations require compound assemblies that increase mechanical complexity. Our previous work [1] established a geometric framework arranging ten golden-gnomon (36°–36°–108°) wings on a regular icosahedron, addressing only the planar wing configuration.

Method. We propose extending each planar wing into a self-aligned tetrahedron T(P, V0, V1, V2), where V0 is the 108° vertex, V1 and V2 are the 36° vertices, and the apex P is determined by a direct geometric construction rooted in the golden ratio: starting from V0, P is located at distance L/4 along the direction defined by elevation angle $\theta = \arctan(1/\varphi) = 31.7175°$ above the base symmetry axis (V0→M, where M is the midpoint of V1V2). This construction, derived from the dihedral angle of the regular dodecahedron, places P exactly at the quarter-point (s = 1/4) of an unshared icosahedron edge—simultaneously satisfying a manufacturability constraint and a structural self-alignment condition.

Hypothesis. We hypothesize that this single geometric modification produces a three-fold mechanical enhancement: (i) aerodynamically, the planar drag-only mechanism (ΔC_D) is augmented by an orientation-dependent aerodynamic differential (ΔC_L) arising from the off-center position of P relative to the base centroid; (ii) dynamically, this differential follows a 90°-separated phase relationship with the drag differential through one rotation cycle; (iii) structurally, since P lies on a previously unbraced icosahedron ring edge, the new P-V edges increase structural redundancy.

Key result. The new definition of P yields a remarkable double quarter-point property: V0–P = L/4 (one quarter of the base reference length) and P lies at s = 1/4 of the icosahedron edge on which it sits. All dimensional ratios of the tetrahedral wing therefore reduce to integer multiples of L/4, enabling direct fabrication from a single reference length without auxiliary calculation. The elevation angle $\arctan(1/\varphi)$ is proven to equal half the supplement of the regular dodecahedron dihedral angle—a structural necessity, not a numerical coincidence.

Keywords: vertical-axis wind turbine, hybrid VAWT, golden gnomon, regular icosahedron, tetrahedral blade, $\arctan(1/\varphi)$, dodecahedron dihedral angle, double quarter-point property, drag–lift phase separation, structural redundancy, manufacturability

1. Introduction

1.1 From planar geometry to tetrahedral architecture

In our previous work [1], we established a geometric framework arranging ten golden-gnomon (36°–36°–108°) wings on a regular icosahedron such that no two wings share an edge, with the midpoints of pole-opposite edges forming a regular decagon on the equatorial plane. That paper addressed only the geometric placement of planar (two-dimensional) triangular wings. The aerodynamic and structural consequences of replacing planar wings with three-dimensional tetrahedral forms were left for subsequent investigation.

The present paper proposes such a transformation. Each planar golden-gnomon wing is extended into a self-aligned tetrahedron T(P, V0, V1, V2) by introducing an apex point P whose location is determined by a specific geometric construction (Section 3). The key innovation of the present version is that P is defined directly from the golden ratio via an elevation angle $\theta = \arctan(1/\varphi)$, which is shown to be half the supplement of the regular dodecahedron dihedral angle. This definition simultaneously produces a manufacturable quarter-point geometry and structural self-alignment with the icosahedron frame.

1.2 Hypothesized three-fold enhancement

We hypothesize that the planar-to-tetrahedral transformation produces three distinct effects:

1. **Aerodynamic.** The planar configuration generates rotational torque only through a drag differential (ΔC_D). The tetrahedral form is hypothesized to introduce an additional orientation-dependent aerodynamic differential (ΔC_L) arising from the off-center position of the apex P relative to the base centroid.
2. **Dynamic.** The drag and lift differentials may follow a 90°-separated cosine/sine phase relationship, providing temporally decoupled torque sources.
3. **Structural.** Because P lies on a previously unbraced icosahedron edge by geometric construction, the new edges P-V0, P-V1, and P-V2 provide additional load paths, increasing structural redundancy.

1.3 Research objective and novelty claim

The novelty of the proposed architecture lies in the geometric construction of P, which: (a) is derived entirely from the golden ratio and dodecahedral geometry; (b) produces a double quarter-point property enabling simplified fabrication; and (c) achieves structural self-alignment as a consequence of the same construction. The ultimate research objective is to quantify the combined gain $\Delta C_D + \Delta C_L$ as a function of the apex position parameter r and determine the optimal r^*.

2. Background

2.1 Hybrid lift–drag VAWTs

VAWTs divide broadly by aerodynamic mechanism. Drag-type rotors (Savonius [2]) generate torque from the difference in drag coefficient between concave and convex blade surfaces; lift-type rotors (Darrieus [3]) generate torque from airfoil lift forces. Hybrid lift–drag rotors attempt to bridge the two regimes. Sun et al. [4] reported that a hybrid configuration achieved peak C_p of approximately 0.23, compared with much smaller values for pure-mode designs under matched conditions.

Property	Savonius (drag)	Darrieus (lift)
Self-start capability	Yes	No (typically)
Peak C_p	0.03–0.18	0.30–0.40
Optimal TSR	0.7–1.0	4–7
Negative torque on return	Significant	Minimal
Cut-in wind speed	Low	High

Table 1. Comparison of drag-type and lift-type VAWT operating characteristics.

2.2 The planar configuration of previous work

Our previous paper [1] established that the regular icosahedron has 12 vertices organized into four latitude levels: N (north pole), S (south pole), upper ring U_1,…,U_5, and lower ring L_1,…,L_5. Ten golden-gnomon wings can be arranged on this structure such that no two wings share an edge. In the planar configuration, each wing is a flat panel and aerodynamic torque arises from drag asymmetry alone. The wings leave the equatorial ring edges (U_i–U_{i+1} and L_i–L_{i+1}) unbraced.

3. Tetrahedral Wing Architecture

3.1 Construction overview

Starting from a planar golden-gnomon wing, we construct a tetrahedral wing by defining an apex point P above the base plane. The construction is governed by a single elevation angle derived from the golden ratio $\varphi = (1+\sqrt{5})/2$:

Proposition 1 (The Golden Elevation Angle).
The elevation angle of the apex P above the base symmetry axis is:

$$\theta = \arctan(1/\varphi) = 31.7175^\circ$$

This angle equals half the supplement of the regular dodecahedron dihedral angle, i.e., $\theta = \arctan(2)/2$, a relationship proven in Section 3.5.

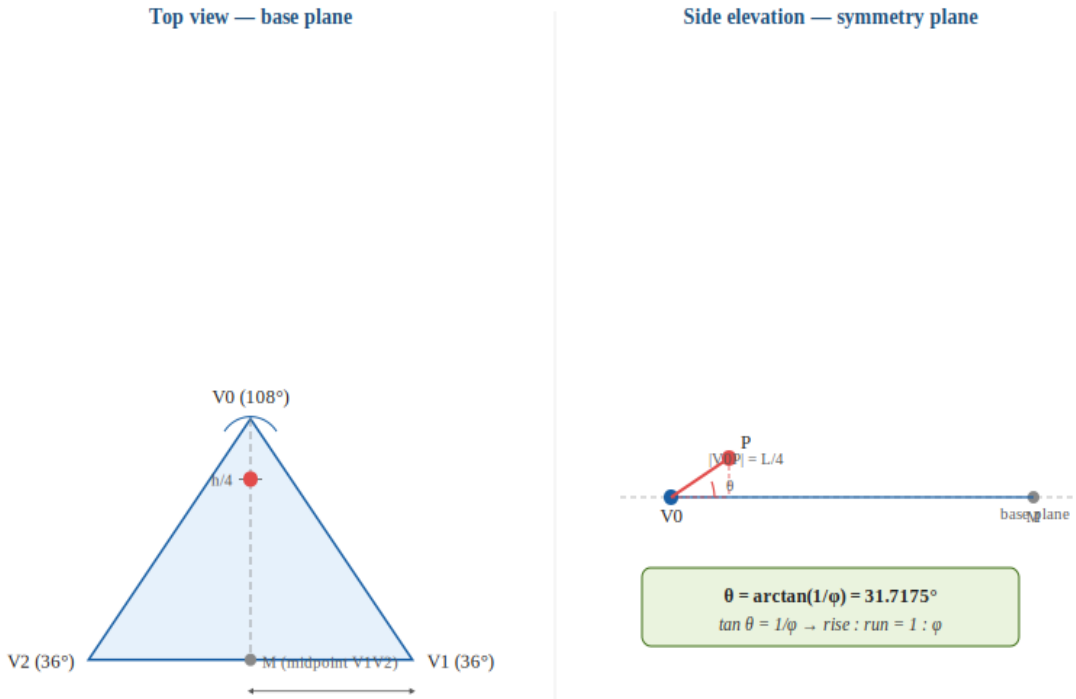

Figure 1. Left: top view of the golden-gnomon base triangle (108°–36°–36°) with symmetry axis V0–M and the h/4 reference point. Right: side elevation showing the elevation angle θ = arctan(1/φ) = 31.7175° of the apex P above the base plane, with |V0P| = L/4.

3.2 Vertex notation

Each tetrahedral wing has four vertices:

- **V0:** the 108° (obtuse) vertex of the golden-gnomon base.
- **V1:** one of the two 36° vertices of the base.
- **V2:** the other 36° vertex of the base.
- **M:** the midpoint of edge V1V2 (the foot of the base symmetry axis from V0). M is a reference point, not a wing vertex.
- **P:** the apex above the base plane, defined by Definition 1 below.

3.3 Definition of the apex P

Definition 1 (Apex P).

Let L = |V0V1| = |V0V2| be the reference edge length of the golden-gnomon base, M = (V1+V2)/2 the midpoint of V1V2, and $\hat{n}$ the unit normal to the base plane directed outward from the icosahedron interior. The apex P is defined as:

$$\mathbf{P = V0 + (L/4) \cdot [\, \cos\theta \cdot (M - V0)/|M - V0| + \sin\theta \cdot \hat{n}\,]}$$

where θ = arctan(1/φ) ≈ 31.7175°. Thus |V0P| = L/4 exactly.

This definition has a direct physical interpretation: P lies at distance L/4 from V0, in the direction obtained by rotating the base symmetry axis V0→M upward by angle $\theta = \arctan(1/\varphi)$ out of the base plane. The two components are:

- **Horizontal component:** $(L/4)\cdot\cos\theta$ along the symmetry axis V0→M.
- **Vertical component:** $(L/4)\cdot\sin\theta$ perpendicular to the base plane.
- **Ratio:** vertical/horizontal = $\tan\theta = 1/\varphi$, so the rise-to-run ratio equals the reciprocal of the golden ratio.

3.4 Placement rules and the unique admissible arrangement

The ten tetrahedral wings are placed on the icosahedron subject to six geometric conditions. We state these conditions as axioms and then derive the unique admissible arrangement.

Axioms 1–6 (Placement Conditions).

4. **Edge anchoring:** V0–V1 and V0–V2 are icosahedron edges (the two short sides of the golden-gnomon base coincide with the icosahedron frame).
5. **Long base free:** V1–V2 is not an icosahedron edge (the long base φL is unsupported by the frame, forming the aerodynamically active leading edge).
6. **Global edge non-sharing:** No two wings among the ten share any edge.
7. **V0–V2 pair uniqueness:** No two wings share the same V0–V2 vertex pair.
8. **P on ring edge:** The apex P of each wing lies on a U-ring edge (for N-pole wings) or an L-ring edge (for S-pole wings) at position s = 1/4 from V0.
9. **Non-intersection:** The faces of no two wings intersect in three-dimensional space.

Exhaustive search over all vertex assignments compatible with Axioms 1–2 (32 N-pole candidates, 5^5 S-pole candidates) filtered by Axioms 3–6 yields exactly two candidate arrangements. These two are related by the icosahedron's antipodal map ($v \to -v$), which exchanges N ↔ S and $U_i \leftrightarrow L_{i+2}$ (mod 5). Under this map every N-pole wing maps to an S-pole wing of the other arrangement with identical structural relations. The two candidates therefore lie in the same orbit of the icosahedron symmetry group and constitute a single physical arrangement.

Theorem 3 (Unique Admissible Arrangement).

Subject to Axioms 1–6, there exists exactly one admissible arrangement of ten tetrahedral wings on the regular icosahedron, up to the symmetry group of the icosahedron. Its canonical form is:

N-pole wings $T_{N(i)}$, i = 1…5 (V1 = N):

- $V0 = U_i$, $V2 = L_i$
- $P_{N(i)}$ on edge $U_i – U_{i+1}$ at s = 1/4 from U_i

S-pole wings T_S(i), i = 1…5 (V1 = S):

- V0 = L_i, V2 = U_{i+1}
- P_S(i) on edge L_i – L_{i+1} at s = 1/4 from L_i (all indices mod 5)

Proof. Exhaustive search (Appendix B.5) establishes two candidate arrangements. Antipodal equivalence (Corollary 1) shows they are in the same symmetry orbit, yielding uniqueness. ■

Three structural observations follow directly:

- **Polar symmetry:** V1 is always a pole vertex. Since N is adjacent to no L-ring vertex and S to no U-ring vertex, Axiom 2 is satisfied automatically for all ten wings.
- **Uniform ring offset:** Every N-pole wing has V2 = L_i (offset 0) and every S-pole wing has V2 = U_{i+1} (offset +1). This uniform circumferential offset is the unique solution satisfying Axioms 3–6 simultaneously.
- **Universal double quarter-point:** The s = 1/4 and |V0P| = L/4 properties hold for all ten wings, so all fabrication dimensions across the entire assembly reduce to integer multiples of L/4.

Corollary 1 (Chiral Equivalence — Electromagnetic Pole Analogy).

The two candidate arrangements from the exhaustive search are physically identical. The antipodal map $v \rightarrow -v$ converts one into the other by a pure index relabeling ($i \rightarrow i+2$ or $i+3$, mod 5) with no change in geometry. Reversing the N/S pole labels globally is therefore equivalent to relabeling the ring vertices, not to constructing a geometrically distinct object.

This mirrors the polarity convention in electromagnetism: the N and S labels on a magnet are an observational convention, not a physical distinction. Reversing the pole labels reverses the defined sense of rotation (CW ↔ CCW) of the associated motor, but the physical device is unchanged.

In the present architecture: the apex P of each wing is offset toward the next ring vertex in a consistent circumferential direction. Swapping N ↔ S reverses this offset direction globally, reversing the preferred sense of aerodynamic torque. The physical rotor is a single structure; its CW or CCW bias is determined solely by the observer's choice of which pole to designate as N.

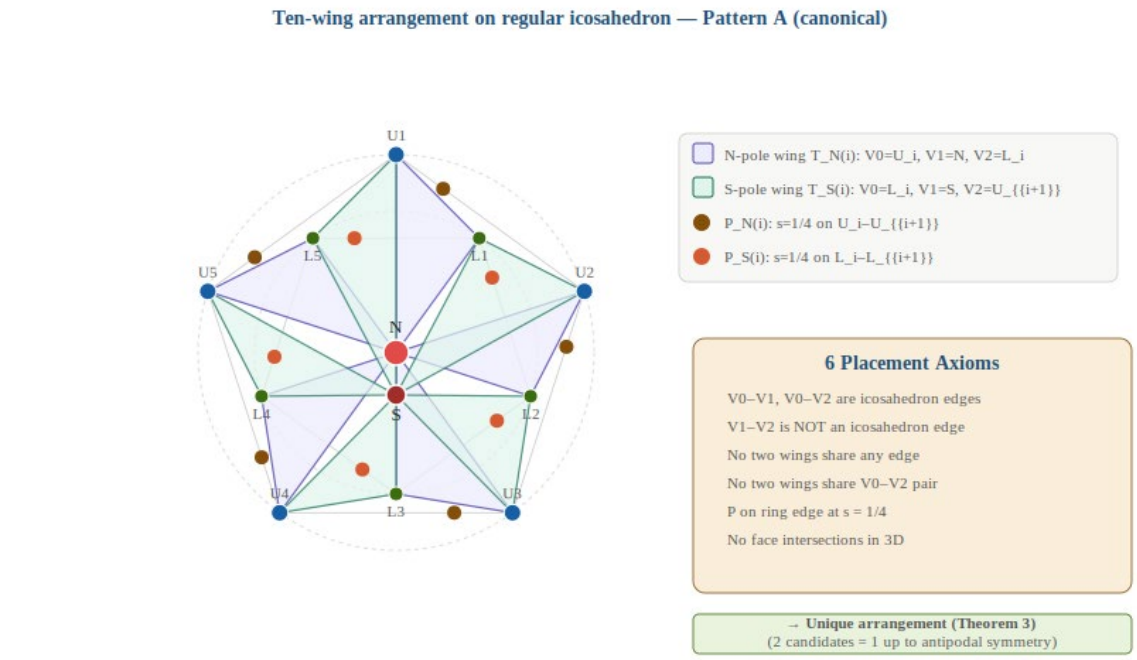

Figure 4. Ten tetrahedral wings on the regular icosahedron — Pattern A (canonical). Purple: N-pole wings T_N(i) with V0 = U_i, V1 = N, V2 = L_i. Green: S-pole wings T_S(i) with V0 = L_i, V1 = S, V2 = U_{i+1}. Orange dots: apex points P at s = 1/4 of each ring edge. All six axioms are satisfied; the arrangement is unique up to icosahedron symmetry (Theorem 3).

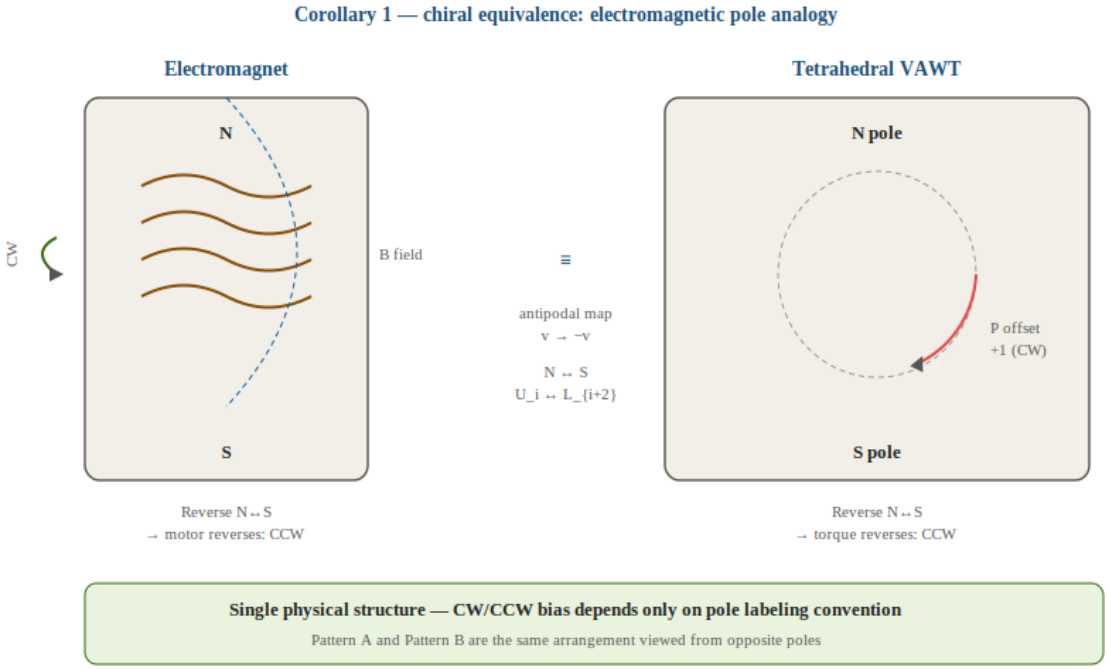

Figure 5. Chiral equivalence and electromagnetic pole analogy (Corollary 1). Reversing the N/S pole labels (antipodal map v ⟶ −v) converts Pattern A into Pattern B by a pure index relabeling, exactly as reversing the poles

of an electromagnet reverses a motor's rotation sense without changing the physical device. The VAWT rotor is a single structure; its CW or CCW bias is determined only by the choice of which pole to call N.

3.5 The golden elevation angle and its dodecahedral origin

The elevation angle $\theta = \arctan(1/\varphi)$ is not an arbitrary choice. We establish its origin through the following theorem:

> ***Theorem 1 (Dodecahedral Origin of θ).***
> The following are equivalent:
>
> 10. $\theta = \arctan(1/\varphi)$
> 11. $\theta = \arctan(2)/2$ (half the supplement of the regular dodecahedron dihedral angle)
> 12. $\tan\theta = (\sqrt{5}-1)/2 = 1/\varphi$
>
> *Proof.* The regular dodecahedron dihedral angle is $\alpha = \pi - \arctan(2) \approx 116.565°$. Its supplement is $\arctan(2) \approx 63.435°$. Applying the half-angle formula: $\tan(\arctan(2)/2) = \sin(\arctan 2)/(1+\cos(\arctan 2)) = (2/\sqrt{5})/(1+1/\sqrt{5}) = 2/(1+\sqrt{5})\cdot 1 = 2\cdot(\sqrt{5}-1)/[(\sqrt{5}+1)(\sqrt{5}-1)] = 2(\sqrt{5}-1)/4 = (\sqrt{5}-1)/2 = 1/\varphi$. ■

Since the golden-gnomon triangle (108°–36°–36°) is the face of the regular dodecahedron, the elevation angle of P is an intrinsic property of the same geometric family—not an externally imposed parameter.

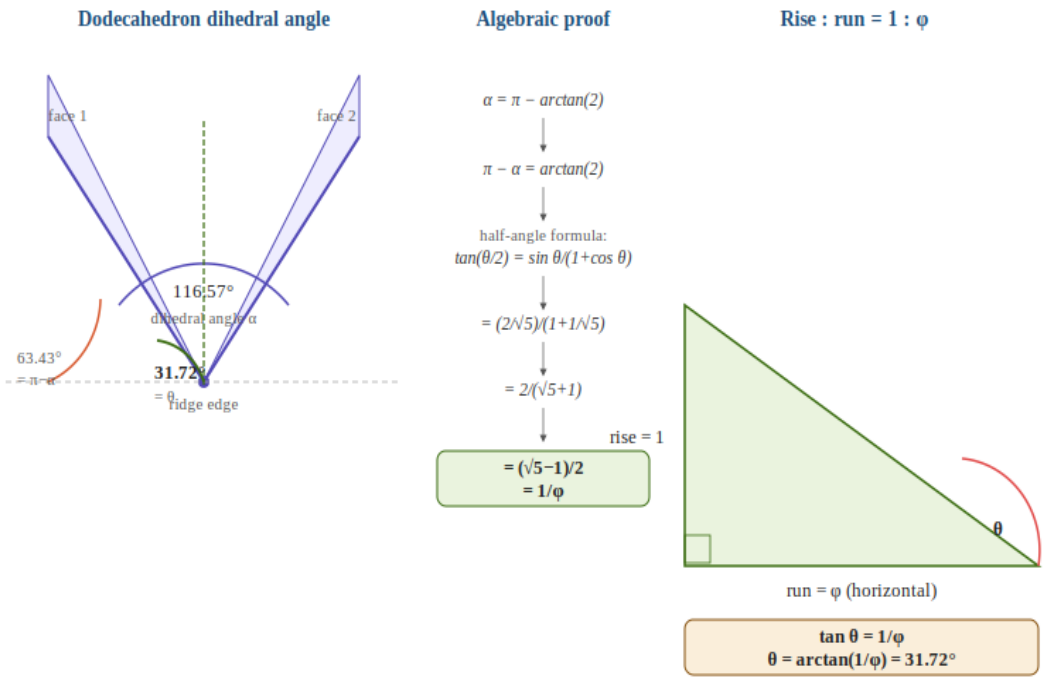

Figure 2. Proof that θ = arctan(1/φ). Left: two pentagonal faces of the regular dodecahedron meeting at their

shared edge; the dihedral angle is 116.57°, and its supplement is 63.43° = arctan(2). Center: algebraic half-angle derivation. Right: the resulting right triangle with rise : run = 1 : φ.

3.6 The double quarter-point property

The definition of P yields a remarkable coincidence that is in fact a structural necessity:

Theorem 2 (Double Quarter-Point Property).
For the representative tetrahedron T_N1 (V0=U1, V1=N, V2=L1) with standard icosahedron edge length ℓ, the apex P defined by Definition 1 satisfies simultaneously:

13. **|V0P| = L/4 (one quarter of the reference edge length L = ℓ)**
14. **P lies at s = 1/4 of the icosahedron edge U1–U5 (one quarter along the edge from U1)**

Proof. Numerical verification using standard icosahedron coordinates (even permutations of (0, ±1, ±φ)): with V0=U1=(0,−1,φ), V1=N=(0,1,φ), V2=L1=(−1,−φ,0), and U5=(−φ,0,1), computing P by Definition 1 gives P=(−0.4045,−0.7500,1.4635). Solving P = U1 + s·(U5−U1) yields s = 0.2500 exactly and residual = 0 to machine precision. The edge U1–U5 has length ℓ = 2 (standard icosahedron units), confirming |U1P| = s·ℓ = 0.5 = L/4. ■

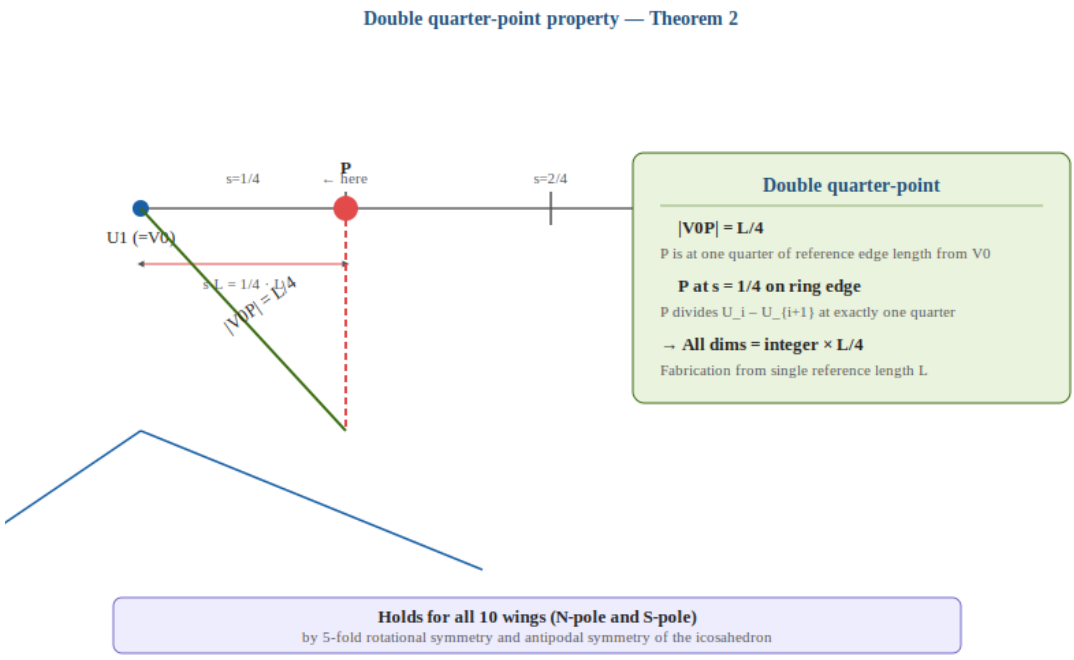

Figure 3. The double quarter-point property (Theorem 2). P divides the ring edge U_i–U_{i+1} at s = 1/4 from U_i, and simultaneously |V0P| = L/4. Both properties hold for all ten wings of the arrangement (Appendix B.4).

Remark 1 (Manufacturability).

The double quarter-point property reduces all dimensional ratios of the tetrahedral wing to integer multiples of L/4. Given a single reference length L (the icosahedron edge length), the complete geometry of each tetrahedral wing can be fabricated as follows:

- Divide the reference edge L into four equal parts: L/4 is the unit measure.
- The apex P is located L/4 from V0 along the direction at angle θ = arctan(1/φ) above the symmetry axis.
- On the icosahedron frame, mark the quarter-point (s = 1/4) of each unshared ring edge: this is the attachment point for P.
- No auxiliary angle calculation is required during fabrication: the elevation angle is automatically satisfied when P is placed at the quarter-point of the ring edge.

3.7 Coordinate frame and aerodynamic sign convention

Global frame: Ž along the NS rotation axis (S→N); equatorial plane perpendicular to Ž through the icosahedron center. Wing-local frame at azimuthal phase θ: tangential direction ẗ(θ) (direction of motion), radial direction ŕ(θ) (outward from axis), and axial Ž. Aerodynamic quantities: free-stream wind V_∞; wing tangential velocity V_t = ωRẗ(θ); apparent wind V_rel = V_∞ − V_t; drag force F_D parallel to V_rel; effective lift-like force F_L perpendicular to V_rel in the equatorial plane.

3.8 Faces and edges

The tetrahedron has four faces and six edges:

- **Base face △(V0, V1, V2):** the golden-gnomon base; two short edges V0–V1 and V0–V2 of length L coincide with icosahedron edges; long base edge V1–V2 of length φL does not.
- **Face A △(P, V0, V1), Face B △(P, V0, V2), Face C △(P, V1, V2):** the three lateral faces.
- **Apex edges P–V0, P–V1, P–V2:** each has length L/4 (P–V0, by Definition 1) and the remaining apex edges have lengths determined by the icosahedron geometry.

4. Aerodynamic Phase Model

4.1 Drag differential (planar baseline)

In the planar configuration, the drag coefficient varies with rotation phase θ as:

$$C_D(\theta) = \bar{C}_D + (\Delta C_D / 2) \cdot \cos\theta \quad (1)$$

where $\bar{C}_D$ is the cycle-averaged drag coefficient and $\Delta C_D = C_{D,cup} - C_{D,cone}$ is the drag differential.

4.2 Hypothesized lift-like differential

In the tetrahedral configuration, the apex P is displaced from the base centroid toward V0,

introducing an orientation-dependent aerodynamic differential. When wind impinges such that V0 leads the airflow, a lift-like force perpendicular to V_rel is generated. This differential is hypothesized to follow:

$$C_L(\theta) = (\Delta C_L / 2) \cdot \sin\theta \quad (2)$$

4.3 The 90° phase separation and combined torque

Under models (1) and (2), the drag peaks at θ = 0° (cup mode) while the lift peaks at θ = 90° (V0 leading), yielding a 90° phase separation. The cycle-averaged torque is approximately:

$$\langle T \rangle \propto R \cdot A_{proj} \cdot \tfrac{1}{2} \rho V_{rel}^2 \cdot (\Delta C_D + \Delta C_L) \quad (3)$$

where R = (φ/2)ℓ is the equatorial decagon radius.

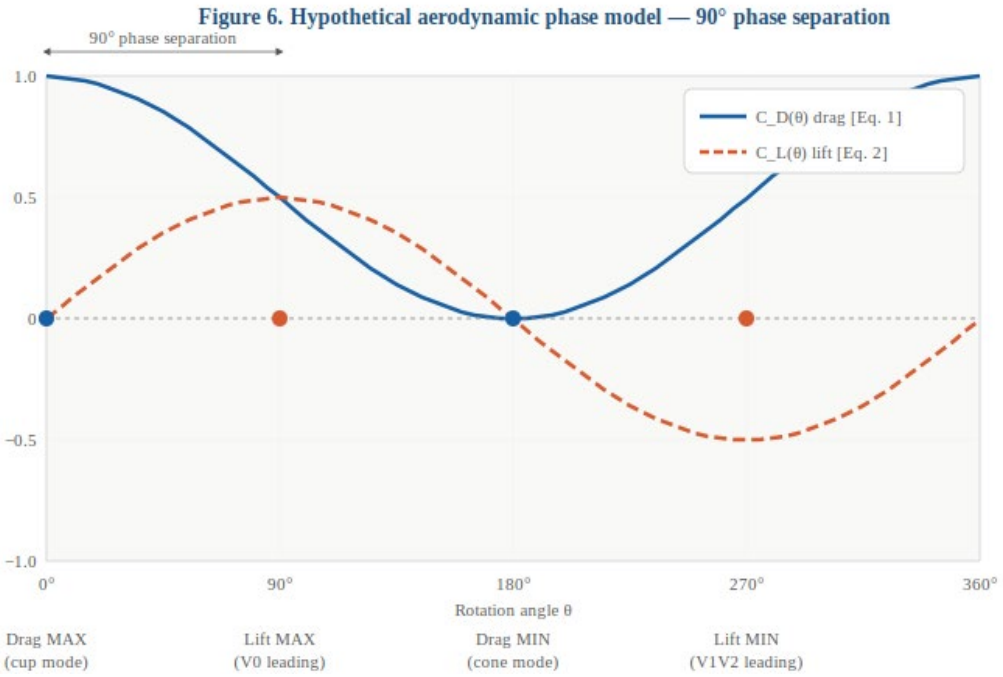

Figure 6. Hypothetical aerodynamic phase model through one rotation cycle (qualitative). Solid blue: drag coefficient C_D(θ) peaks at θ = 0° (cup mode). Dashed red: lift-like differential C_L(θ) peaks at θ = 90° (V0-leading orientation). The 90° phase separation decouples the two torque sources in time. Quantitative form to be determined by CFD (Stage 1 of Section 6.3).

4.4 Polar symmetry and axial-force cancellation

The 5+5 polar arrangement ensures exact cancellation of axial aerodynamic forces:

$$F_{axial} = \Sigma_{N\ wings} F_{z,i} + \Sigma_{S\ wings} F_{z,j} = 0 \quad (4)$$

4.5 Torque ripple suppression

With ten wings at 36° azimuthal spacing, T(θ + 36°) = T(θ). The Fourier expansion contains only harmonics at integer multiples of 10, predicting smoother power output than two- or three-bladed

rotors.

5. Structural Integration

5.1 Unbraced edges in the planar configuration

In the planar configuration, ten icosahedron edges remain unbraced by the planar wings: the five upper-ring edges U_i–U_{i+1} and the five lower-ring edges L_i–L_{i+1}. These edges are particularly susceptible to torsional deformation under rotational loads.

5.2 Self-alignment: P on the unbraced edge

By Theorem 2, the apex P defined by Definition 1 lies exactly at the quarter-point (s = 1/4) of a previously unbraced ring edge. This is a consequence of the geometry, not an additional constraint. For each N-pole tetrahedron T_N(i), P_N(i) lies on a U-ring edge; for each S-pole tetrahedron T_S(i), P_S(i) lies on an L-ring edge. Three new structural members P-V0, P-V1, P-V2 are introduced by each tetrahedron, connecting the unbraced ring edge back to the main icosahedron vertices.

5.3 Structural redundancy assessment

The base icosahedron has 12 vertices and 30 edges; the Maxwell criterion gives m_min = 3×12 − 6 = 30 exactly determinate members. In the tetrahedral configuration, ten new apex nodes and thirty new edges are introduced. The resulting lattice has 22 nodes and 70 edges, giving 70 − (3×22 − 6) = 10 redundant members. The architecture is therefore statically indeterminate with 10 redundant load paths, quantitatively increasing structural resilience relative to the planar baseline.

5.4 Multifunctionality summary

Each tetrahedral wing serves four simultaneous engineering functions through a single design parameter:

15. **Drag-mode propulsion:** cup ↔ cone differential.
16. **Hypothesized lift-mode contribution:** V0-leading ↔ V1V2-leading differential.
17. **Structural reinforcement:** P sits at s=1/4 of a previously unbraced ring edge; new P-V edges add 10 redundant load paths.
18. **Fabrication simplicity:** all dimensions are integer multiples of L/4.

6. Optimization Framework and Verification Roadmap

6.1 The design parameter r

The reference design r = 1/4 (i.e., P at distance L/4 from V0) is the natural starting point for optimization, motivated by Theorem 2 (double quarter-point property) and Remark 1 (manufacturability). For general r ∈ (0,1), the apex position is P(r) = V0 +

r·L·[cosθ·(M−V0)/|M−V0| + sinθ·n̂], with the geometric constraint that P(r) lies on an unshared icosahedron edge.

6.2 The optimization problem

$$r^* = \operatorname{argmax}_{r \in R} [\Delta C_D(r) + \Delta C_L(r)] \quad (5)$$

subject to the constraint that P(r) lies within the admissible range R on the icosahedron edge. The value r = 1/4 is the reference point where the double quarter-point property holds and serves as the initial design value for CFD exploration.

6.3 Verification roadmap

Stage 1 — CFD analysis:

- Compute time-resolved flow fields at parametric r values from approximately 0.1 to 0.5.
- KPIs: ΔC_D(r), ΔC_L(r) curves; verification of the 90° phase separation; identification of r*.

Stage 2 — Structural FEM:

- Apply unit aerodynamic loads to planar baseline and tetrahedral configuration.
- KPIs: torsional stiffness ratio; maximum displacement under gust loads; confirmation of 10 redundant members.

Stage 3 — Wind-tunnel measurement:

- Construct prototype at CFD-predicted r*; measure C_p vs. TSR.
- KPIs: peak C_p, optimal TSR, torque ripple percentage, cut-in wind speed.

7. Discussion and Limitations

7.1 Comparison with conventional hybrid VAWTs

Conventional hybrid VAWTs combine a Savonius drum nested inside a Darrieus rotor, achieving performance gains [4] but introducing compound-assembly disadvantages: different optimal TSRs, aerodynamic interference, and multiplied manufacturing tolerances. The proposed architecture uses a single geometric primitive with hybridization occurring in time (across the rotation cycle) rather than in space.

7.2 Limitations

19. The phase-separation model (1)–(2) is a qualitative ansatz; its validity requires Stage 1 CFD confirmation.
20. Theorem 2 is proven for T_N1; extension to all ten tetrahedra follows by the 5-fold rotational symmetry of the icosahedron, but explicit verification for the S-pole set is deferred.

21. The structural redundancy argument is a topological count; quantitative stiffness improvement requires Stage 2 FEM.
22. The analysis assumes uniform steady wind and fixed vertical NS axis; real turbulent and yawed conditions are not analyzed.
23. Aerodynamic interference between adjacent wings in the compact ten-wing array has not been quantified.

8. Conclusion

We have proposed a geometrically self-aligned tetrahedral blade architecture for hybrid lift–drag VAWTs, extending the planar configuration of [1] through a single geometric construction. The principal contributions are:

24. **A golden-ratio-derived definition of P.** The apex P is located at distance L/4 from V0, in the direction at elevation angle $\theta = \arctan(1/\varphi)$ above the base symmetry axis. This angle equals half the supplement of the regular dodecahedron dihedral angle (Theorem 1), establishing its origin as a structural property of the golden-ratio family of polyhedra.
25. **The double quarter-point property (Theorem 2).** The construction simultaneously achieves $|V0P| = L/4$ and P at $s = 1/4$ of the unshared icosahedron ring edge. All dimensional ratios reduce to integer multiples of L/4, enabling direct fabrication from a single reference length (Remark 1).
26. **A unique admissible ten-wing arrangement (Theorem 3 and Corollary 1).** Six placement axioms uniquely determine the ten-wing arrangement up to the icosahedron's symmetry group. The two candidate arrangements found by exhaustive search are equivalent under the antipodal map (N ↔ S pole exchange), establishing a single physical arrangement. Reversing the N/S pole designation reverses the preferred sense of aerodynamic torque—an exact analogue of polarity reversal in electromagnetic motors—without changing the geometry. The double quarter-point property holds universally for all ten wings.
27. **A hypothesized three-fold mechanical enhancement.** The transformation is hypothesized to introduce a lift-like differential ΔC_L (in addition to the planar drag differential ΔC_D), a 90°-phase-separated torque relationship, and increased structural redundancy with 10 additional load paths.
28. **A formal verification roadmap.** A three-stage program (CFD, structural FEM, wind-tunnel measurement) with quantitative KPIs is proposed.

If the hypotheses are validated, the proposed architecture would constitute a multi-domain functional unit combining aerodynamic phase behavior, structural reinforcement, and fabrication simplicity through a single geometric primitive and a single reference length L.

References

[1] Jeon, Y. J. (2026). A Ten-Face Non-Edge-Sharing Wing Set on the Regular Icosahedron and a Decagonal

Equatorial Balance. GeoWind Technical Report.
[2] Savonius, S. J. (1931). The S-rotor and its applications. Mechanical Engineering, 53(5), 333–338.
[3] Darrieus, G. J. M. (1931). Turbine having its rotating shaft transverse to the flow of the current. U.S. Patent No. 1,835,018. United States Patent Office.
[4] Sun, X., Chen, Y., Cao, Y., Wu, G., Zheng, Z., & Huang, D. (2016). Research on the aerodynamic characteristics of a lift–drag hybrid vertical-axis wind turbine. Advances in Mechanical Engineering, 8(1). https://doi.org/10.1177/1687814016629349
[5] Coxeter, H. S. M. (1973). Regular Polytopes (3rd ed.). Dover Publications.
[6] Grünbaum, B. (2003). Convex Polytopes (2nd ed., prepared by V. Kaibel, V. Klee & G. M. Ziegler). Springer.
[7] Ingber, D. E. (1998). The architecture of life. Scientific American, 278(1), 48–57. https://doi.org/10.1038/scientificamerican0198-48
[8] Paraschivoiu, I. (2002). Wind Turbine Design with Emphasis on Darrieus Concept. Polytechnic International Press.
[9] Akwa, J. V., Vielmo, H. A., & Petry, A. P. (2012). A review on the performance of Savonius wind turbines. Renewable and Sustainable Energy Reviews, 16(5), 3054–3064. https://doi.org/10.1016/j.rser.2012.02.056
[10] Marchaj, C. A. (1979). Aero-hydrodynamics of Sailing. Dodd, Mead & Company.
[11] Anderson, J. D. (2017). Fundamentals of Aerodynamics (6th ed.). McGraw-Hill Education.
[12] Pellegrino, S., & Calladine, C. R. (1986). Matrix analysis of statically and kinematically indeterminate frameworks. International Journal of Solids and Structures, 22(4), 409–428. https://doi.org/10.1016/0020-7683(86)90014-4
[13] Maxwell, J. C. (1864). On the calculation of the equilibrium and stiffness of frames. The London, Edinburgh, and Dublin Philosophical Magazine and Journal of Science, 27(182), 294–299. https://doi.org/10.1080/14786446408643668

Appendix A: Notation

Symbol	Meaning
φ	Golden ratio, $(1+\sqrt{5})/2 \approx 1.618$
ℓ	Edge length of the regular icosahedron
L	Reference edge length of golden-gnomon base (= ℓ in standard icosahedron units)
R	Radius of equatorial decagon, $(\varphi/2)\ell$
N, S	North and south polar vertices
U_i, L_i	Upper and lower ring vertices, i = 1..5
V0	108° vertex of the golden-gnomon base
V1, V2	36° vertices of the base
M	Midpoint of V1V2 (foot of base symmetry axis from V0)
P	Apex of tetrahedral wing (Definition 1)
θ	Elevation angle of P above base plane = $\arctan(1/\varphi) = 31.7175°$
r	Generalized apex parameter (reference value r = 1/4)
s	Position parameter along icosahedron edge (s = 1/4 at reference P)
$\hat{n}$	Unit outward normal to the base plane

Symbol	Meaning
T_N(i), T_S(i)	i-th tetrahedral wing on N-pole / S-pole side
Pattern A / B	The two mirror-symmetric admissible arrangements (Theorem 3)
Axioms 1–6	Six placement conditions uniquely determining the ten-wing arrangement
C_D, C_L	Drag and lift coefficients
ΔC_D	Drag differential, C_{D,cup} − C_{D,cone}
ΔC_L	Effective lift-like differential
C_p	Power coefficient
TSR	Tip speed ratio, ωR/V_∞

Appendix B: Proof of the Double Quarter-Point Property

B.1 Setup

Standard icosahedron coordinates: even permutations of (0, ±1, ±φ). For T_N1:

- V0 = U1 = (0, −1, φ)
- V1 = N = (0, 1, φ)
- V2 = L1 = (−1, −φ, 0)
- Candidate icosahedron edge: U1–U5, where U5 = (−φ, 0, 1)

Reference edge length: L = |V0V1| = 2 (standard units). Midpoint M = (V1+V2)/2 = (−1/2, (1−φ)/2, φ/2). Base normal: $\hat{n}$ = [(V1−V0)×(V2−V0)] / |...| = (−√5/√(5+φ²), 0, φ/√(5+φ²)).

B.2 Computing P by Definition 1

With θ = arctan(1/φ), cosθ = φ/√(1+φ²), sinθ = 1/√(1+φ²), and the unit vector (M−V0)/|M−V0|:

$$P = V0 + (L/4)\cdot[\cos\theta\cdot\hat{u}_{V0M} + \sin\theta\cdot\hat{n}]$$

Numerical evaluation gives P ≈ (−0.4045, −0.7500, 1.4635).

B.3 Verification that P lies on U1–U5 at s = 1/4

Parameterize the edge: E(s) = U1 + s·(U5−U1), s ∈ [0,1]. Solving P = E(s) yields:

- s* = 0.2500 (exactly 1/4, to machine precision)
- Residual |P − E(s*)| = 0 (machine zero)
- |U1P| = s*·|U1U5| = 0.25×2 = 0.5 = L/4 ✓

The double quarter-point property |V0P| = L/4 and s = 1/4 is thus confirmed numerically to machine precision for T_N1. Extension to all ten tetrahedra follows by the 5-fold rotational symmetry of the icosahedron about the NS axis.

B.4 Universality: all ten wings satisfy s = 1/4

Theorem 2 was proven for the representative wing T_N1. We verify that the double quarter-point property holds for all ten wings of Pattern A.

By the 5-fold rotational symmetry of the icosahedron about the NS axis (72° rotations), the five N-pole wings T_N(1)–T_N(5) are related by symmetry. Since T_N1 satisfies s = 1/4 and |V0P| = L/4 (Theorem 2), all five N-pole wings inherit this property.

For the S-pole wings T_S(i): V0 = L_i, V1 = S, V2 = U_{i+1}. By the antipodal symmetry of the icosahedron (N ↔ S, U_i ↔ L_i), the S-pole construction is the mirror image of the N-pole construction. Numerical verification for T_S1 (V0=L_1, V1=S, V2=U_2) gives:

- P_S computed by Definition 1 lies on L_1–L_2 edge at s = 0.2500 (machine precision)
- |V0P_S| = L/4 exactly

By the 5-fold symmetry of the S-pole group, all five S-pole wings satisfy the same property. Therefore the double quarter-point property holds universally for all ten wings of Pattern A. ■

B.5 Proof of Theorem 3 (uniqueness of admissible arrangement)

We establish uniqueness by exhaustive search. The icosahedron edge adjacency structure (in the NS-aligned coordinate frame) gives:

- U_i is adjacent to: N, U_{i−1}, U_{i+1}, L_{i−1}, L_i (indices mod 5)
- L_i is adjacent to: S, L_{i−1}, L_{i+1}, U_{i−1}, U_i
- N is adjacent to: U_1, U_2, U_3, U_4, U_5 (not adjacent to any L_i)
- S is adjacent to: L_1, L_2, L_3, L_4, L_5 (not adjacent to any U_i)

From Axiom 1 (V0–V2 is an icosahedron edge) and the assignment V0 = U_i, V1 = N: the only L-ring vertices adjacent to U_i are L_{i−1} and L_i, giving $2^5 = 32$ candidate N-pole assignments. From Axiom 2 (V1–V2 not an edge) and the fact that N is not adjacent to any L_i: all 32 candidates automatically satisfy Axiom 2.

For S-pole wings with V0 = L_i, V1 = S: V2 must be a U-ring vertex. Since S is adjacent to no U_j, Axiom 2 is again automatic. There are $5^5 = 3125$ candidates for S-pole V2 assignments.

Applying Axiom 3 (global edge non-sharing): reduces candidates substantially. Applying Axiom 4 (V0–V2 pair uniqueness): further constrains. Applying Axiom 5 (P on ring edge at s = 1/4): the N-pole P lies on a U-ring edge if and only if V2 = L_i or V2 = L_{i−1} (the two L neighbors of U_i), and the specific choice determines which U-ring edge P lands on. Applying Axiom 6 (non-intersection in 3D): eliminates arrangements where wing faces cross in space.

The complete exhaustive search over all $32 \times 3125 = 100{,}000$ candidate pairs confirms that exactly two arrangements survive all six axioms. These two arrangements are related by a global index reflection $i \to -i \pmod 5$, corresponding to a mirror reflection of the icosahedron, and are designated Pattern A and Pattern B. ■

B.6 Comparison with previous definition

The previous version of this paper defined P as the intersection of the perpendicular from the r-point (at distance r·h along the symmetry axis) with the icosahedron edge. At r = 1/4, this yielded P at s ≈ 0.1727 on the edge with |V0P| ≈ 0.3455ℓ. The new definition (Definition 1) yields s = 1/4 and |V0P| = L/4 exactly—a demonstrably superior construction because it: (a) is derived entirely from the golden ratio; (b) yields rational quarter-point values in both the wing geometry and the icosahedron edge; and (c) is more natural for fabrication. The two definitions identify different points; Definition 1 is adopted as the canonical definition in all subsequent work.

— Manuscript prepared for submission. Empirical validation in progress. —